The Interplay between Transpiration and Runoff Formulations in Land Surface Schemes Used with Atmospheric Models

RANDAL D. KOSTER

Hydrological Sciences Branch, Laboratory for Hydrospheric Processes, NASA/Goddard Space Flight Center, Greenbelt, Maryland

P. C. D. MILLY

U.S. Geological Survey, Geophysical Fluid Dynamics Laboratory/NOAA, Princeton, New Jersey

(Manuscript received 1 July 1996, in final form 20 November 1996)

ABSTRACT

The Project for Intercomparison of Land-surface Parameterization Schemes (PILPS) has shown that different land surface models (LSMs) driven by the same meteorological forcing can produce markedly different surface energy and water budgets, even when certain critical aspects of the LSMs (vegetation cover, albedo, turbulent drag coefficient, and snowcover) are carefully controlled. To help explain these differences, the authors devised a monthly water balance model that successfully reproduces the annual and seasonal water balances of the different PILPS schemes. Analysis of this model leads to the identification of two quantities that characterize an LSM's formulation of soil water balance dynamics: 1) the efficiency of the soil's evaporation sink integrated over the active soil moisture range, and 2) the fraction of this range over which runoff is generated. Regardless of the LSM's complexity, the combination of these two derived parameters with rates of interception loss, potential evaporation, and precipitation provides a reasonable estimate for the LSM's simulated annual water balance. The two derived parameters shed light on how evaporation and runoff formulations interact in an LSM, and the analysis as a whole underscores the need for compatibility in these formulations.

1. Background

The overall goal of the Project for Intercomparison of Land-surface Parameterization Schemes (PILPS) is to compare the numerous land surface models (LSMs) that are currently used with atmospheric general circulation models (GCMs) and mesoscale models (Henderson-Sellers et al. 1993) and to understand any differences found in their behavior. In the initial phase of PILPS, land surface modelers were provided with a common set of soil and vegetation physical characteristics and a full year of GCM-generated meteorological forcing for two land surface biomes (tropical forest and a grassland) and were asked to generate surface energy and water balances for each. The salient result was the wide disparity in the balances generated by the different schemes (Pitman et al. 1993).

This disparity is not surprising given the numerous model-specific parameterizations that comprise a typical LSM. In fact, the interactions among the components of an LSM are so complex that isolating and quantifying a given component's contribution to the disparity is very difficult. Partly for this reason, PILPS participants were asked to perform some supplemental simulations that imposed further controls on certain processes. In the most tightly controlled of these simulations, the LSMs used common, prescribed values of vegetation coverage, albedo, and surface-to-air bulk transfer coefficients for heat and vapor. In effect, further controls were imposed in the tropical forest version of this experiment relative to the grassland version because the former avoided intermodel differences in snow formulation and in the seasonal variation of surface characteristics, such as leaf-area index.

The tropical forest version of this tightly controlled experiment has been referred to in PILPS documentation as ''TRF-HAR'' (with ''TRF'' denoting tropical forest, ''H'' denoting homogeneous vegetation, ''A'' denoting fixed albedo, and ''R'' denoting fixed transfer coefficients). Figure 1 shows the annual evaporation produced for TRF-HAR by the different PILPS participants (Table 1). In spite of the added controls, the evaporation, which is a key term in both the water and energy balances, still varies significantly among the LSMs. The annual evaporation has a standard deviation of 0.79 mm day^{-1}, equivalent to 22 W m^{-2}.

This degree of intermodel variability has persisted into more recent phases of PILPS, which focus on testing LSM outputs against observations (e.g., Chen et al.

Corresponding author address: Dr. Randal D. Koster, Hydrological Sciences Branch, NASA/GSFC, Code 974, Greenbelt, MD 20771.
E-mail: randal.koster@gsfc.nasa.gov

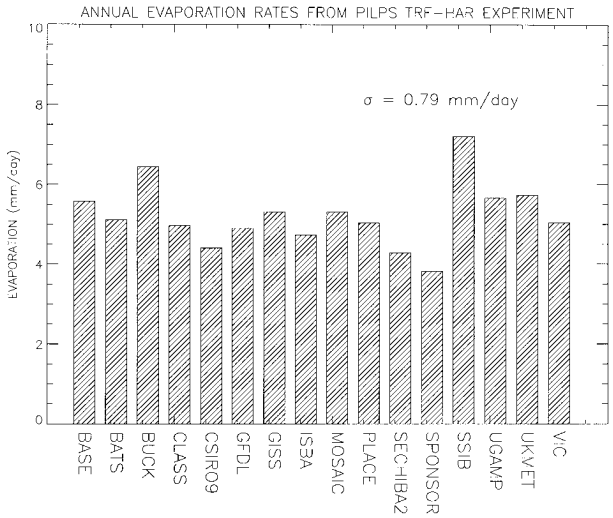

FIG. 1. Evaporation rates for the PILPS TRF-HAR experiment as generated by sixteen LSMs. (See the note regarding SSIB's value in section 4b.)

1997). Several recent PILPS analyses have, in fact, made strides toward explaining this variability. Chen et al. (1997), for example, studied 23 LSMs forced with observations at the Cabauw site in the Netherlands and found that the ranges of simulated annual fluxes were approximately halved upon exclusion of three LSMs that do not impose stomatal resistance under non-water-stressed conditions. Wetzel et al. (1996), studying 14 LSMs forced with observations from the HAPEX-Mobilhy site in France, found that intermodel differences in predicted drainage and bare soil evaporation led to important differences in simulated soil moisture and thus in the simulated water balance. Several recent studies outside the direct purview of PILPS (e.g., Cuenca et al. 1996; Polcher et al. 1996; Shmakin et al. 1996) have also contributed to our understanding of LSM behavior, showing, for example, how LSMs respond to variations in the treatment of surface evaporative resistance, soil moisture transport, and soil moisture heterogeneity.

The sources of variability in LSM behavior, however, are by no means fully resolved. In this paper, we address the problem by going back to the older TRF-HAR experiment with its many imposed controls. We will show that these controls expose to view the critical interactions between evaporation and runoff processes in an LSM, interactions that are responsible for much of the variability in Fig. 1 and that are still present when the controls are removed.

In examining these interactions, we do not focus on details in the parameterizations of runoff and evaporation in the LSMs. Given the diversity and complexity of LSM formulations, a process-by-process comparison can quickly become unmanageable. Rather, we estimate and compare the overall, effective functional behavior of the parameterizations, particularly in terms of how runoff and evaporation vary with soil moisture. Our approach to model analysis and intercomparison is thus consistent with the view espoused by Henderson-Sellers et al. (1993) in an early phase of PILPS: ''It is probably pointless to seek validation of all the parameters that might or might not be in a given land surface parameterization. Rather, it is important to identify the basic functions of the treatment . . .. From the viewpoint of climate modeling, validation of these basic functions . . . on the spatial scale resolved by the model is an important goal.'' We employ as a basis for analysis a simple monthly water balance model, or MWBM. Because the MWBM mimics, at the monthly timescale, the effects of precipitation, potential evaporation, and interception loss on soil water storage, evaporation, and runoff within the different LSMs, its simple structure can be used as a framework for comparing them.

We describe the MWBM in section 2 and use it to analyze the TRF-HAR results in section 3. Section 4 extends the results into a general discussion on the modeling of evaporation and runoff processes in LSMs.

TABLE 1. Fitted MWBM parameters for each LSM.

Model	Reference (if available)	w_β	m_β	w_R	m_R	w_{G1}	m_{G1}	w_{G2}	m_{G2}
BASE	Desborough (1997)	545.	0.0017	689.	0.0076	519.	0.0078	716.	0.118
BATS	Dickinson et al. (1993)	577.	0.0018	588.	0.0036	702.	0.011	709.	0.14
BUCK	Robock et al. (1995)	436.	0.0059	0.	0.	443.	0.021	483.	0.085
CLASS	Verseghy et al. (1993)	479.	0.00099	0.	0.	536.	0.0061	602.	0.071
CSIRO9	Kowalczyk et al. (1991)	731.	0.0026	791.	0.0077	764.	0.0084	834.	0.144
GFDL		431.	0.0014	0.	0.	535.	0.0023	662.	0.487
GISS	Abramopoulos et al. (1988)	296.	0.00042	756.	0.21	3307.	0.00041	719.	0.311
ISBA	Noilhan and Planton (1989)	509.	0.00075	792.	0.014	610.	0.0042	727.	0.066
MOSAIC	Koster and Suarez (1996)	323.	0.0025	195.	0.0021	413.	0.042	458.	0.147
PLACE	Wetzel and Boone (1995)	696.	0.0015	833.	0.023	1156.	−0.0005	0.	0.
SECHIBA2	Ducoudre et al. (1993)	440.	0.0019	535.	0.023	0.	0.0	0.	0.
SPONSOR	Shmakin et al. (1993)	445.	0.0035	446.	0.0074	0.	0.0	0.	0.
SSIB	Xue et al. (1991)	579.	0.0043	0.	0.	519.	−0.028	664.	0.293
UGAMP	Gedney (1995)	456.	0.0020	635.	0.0061	467.	0.0032	595.	0.112
UKMET	Gregory and Smith (1994)	345.	0.00073	0.	0.	727.	0.0080	707.	0.259
VIC	Liang et al. (1994, 1996)	562.	0.0018	466.	0.0011	440.	0.0043	665.	0.049

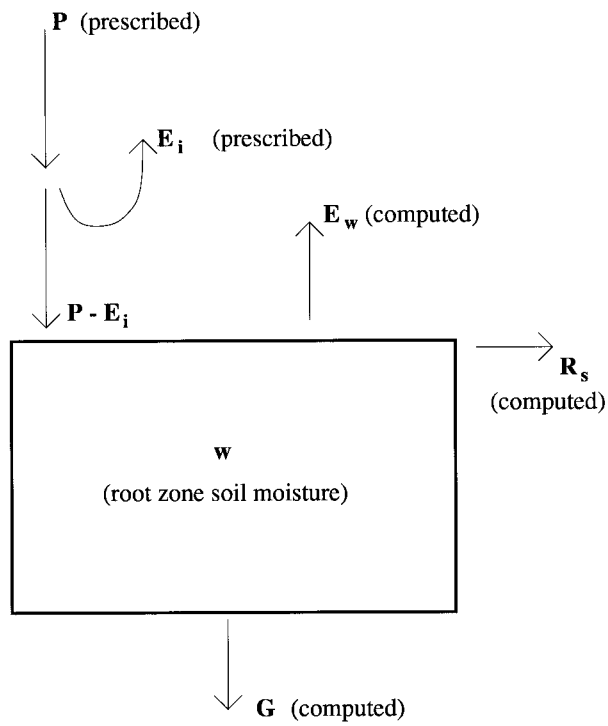

FIG. 2. Components of the MWBM.

2. Monthly water balance model

a. Structure of the MWBM

The MWBM's single prognostic variable is the amount of moisture, w, in the root zone. The MWBM performs no energy balance calculation; radiation forcing and surface temperature are implicitly included through monthly potential evaporation, which, along with precipitation, is used to force the model. The model uses a one-month time step.

A schematic of the MWBM is provided in Fig. 2. The model is forced with a monthly precipitation total, P. A prescribed amount of this water, E_i, is assumed to collect on the canopy leaves or ground litter and evaporate within the month (interception loss); the amount of water applied to the soil during the month is thus $P - E_i$. Of this water, an amount, R_s, runs directly off the surface, and the remainder infiltrates the soil. The root zone soil moisture w increases with this infiltration but decreases through an evaporation, E_w, that represents the sum of transpiration and bare soil evaporation. Water exchange with soil below the root zone (G) also affects w. We refer to G as root-zone drainage, since it is typically positive (i.e., directed downward); in some LSMs, however, G can take on negative values, implying upward flow, or "recharge."

The balance of water in the MWBM is expressed as

$$\frac{w^{(n)} - w^{(n-1)}}{\Delta t} = P^{(n)} - E_i^{(n)} - R_s^{(n)} - G^{(n)} - E_w^{(n)}, \quad (1)$$

with

$$R_s^{(n)} = R[w^{(n)}][P^{(n)} - E_i^{(n)}], \quad (2)$$

$$G^{(n)} = G[w^{(n)}], \quad (3)$$

and

$$E_w^{(n)} = \beta_T[w^{(n)}][E_p^{(n)} - E_i^{(n)}]. \quad (4)$$

Here, the superscript (n) indicates a value for month n, R is the fraction of the throughfall that becomes surface runoff (the "runoff fraction"), β_T is an evaporation efficiency, E_p is the average potential evaporation rate [equivalent to the "wet-surface" rate described by Sud and Fennessey (1982) and Milly (1992); see section 2b], and Δt is the duration of the month. Notice that β_T, R, and G are each functions of the updated soil moisture content, implying an implicit calculation.

In the MWBM, the runoff fraction is a simple function of root zone water content:

$$R(w) = \begin{cases} 0 & R^*(w) < 0 \\ R^*(w) & 0 < R^*(w) < 1 \\ 1 & 1 < R^*(w), \end{cases} \quad (5)$$

where

$$R^*(w) = m_R(w - w_R). \quad (6)$$

The terms m_R (mm^{-1}) and w_R (mm) are prescribed constants.

The exchange of water between the root zone and lower soil layers, G, is usually described in an LSM in terms of a potential gradient and a hydraulic conductivity that increases nonlinearly with soil wetness. In many LSMs, the potential gradient is fixed by gravity, and G can only be positive; in others, moisture conditions below the root zone are tracked and can generate upward flow when the root zone becomes sufficiently dry. To cover the major possibilities, the MWBM uses the following expression for G:

$$G(w) = \begin{cases} m_{G1}(w - w_{G1}) & w < w_{G2} \\ m_{G2}(w - w_{G2}) & w_{G2} < w, \end{cases} \quad (7)$$

where m_{G1} (s^{-1}), w_{G1} (mm), m_{G2} (s^{-1}), and w_{G2} (mm) are prescribed constants.

The sum of transpiration and bare soil evaporation, or E_w, proceeds below the potential rate in many LSMs due to the resistances imposed by vegetation and soil on moisture transfer. The MWBM accounts for this reduction through an efficiency factor, β_T, which is a very simple function of soil moisture:

$$\beta_T = \begin{cases} 0 & \beta_T^* < 0 \\ \beta_T^* & 0 < \beta_T^* < 1 \\ 1 & 1 < \beta_T^* \end{cases} \quad (8)$$

and

$$\beta_T^* = m_\beta(w - w_\beta), \quad (9)$$

where m_β (mm^{-1}) and w_β (mm) are prescribed constants. The slope m_β is positive to reflect the increase in the

ease of transpiration and bare soil evaporation as soil moisture increases. In some LSMs, β_T plateaus at some value less than one when the soil is sufficiently wet. Because the PILPS LSMs' monthly diagnostics do not show, in general, any clear ''leveling off'' of β_T at high w, it is neglected here (though, of course, β_T is not allowed to exceed 1).

Because the PILPS output diagnostics do not provide the information needed to characterize a given LSM's formulation of canopy interception, the MWBM prescribes rather than predicts interception loss for each month. Thus, the MWBM is fully defined by prescribed interception loss rates and simple functions that relate forcing (precipitation and potential evaporation) and root zone soil moisture to surface runoff, drainage, and evaporation.

The specific values used for the functions' parameters are derived for each LSM through an objective curve-fitting procedure (see appendix); overall MWBM input-output response is not tuned. An objective estimation is, of course, critical to a fair test of the MWBM's performance. We must emphasize, though, that the curve fitting implies some limitation to the ''physical'' interpretation of MWBM parameters. The MWBM captures only in the broadest sense the manner in which transpiration and runoff rates increase with increasing soil moisture in a given LSM. Indeed, the derived value of any MWBM parameter generally represents the net effect of several interacting hydrological processes. Through the curve-fitting exercise, the MWBM effectively accounts for these processes without parameterizing them individually.

b. Test of the MWBM

In this section, we test the ability of the relatively simple MWBM to reproduce the water-balance responses of the different PILPS LSMs, in particular their seasonal and annual evaporation rates. A separate set of MWBM parameter values (m_β, w_β, m_R, w_R, m_{G1}, w_{G1}, m_{G2}, and w_{G2}) was derived for each LSM from the equilibrium-year monthly diagnostics generated in the TRF-HAR experiment (see appendix). Table 1 lists these values.

Having determined parameter values for a given LSM, we integrated (1) for 5 yr by repetition of a single year of forcing. All of our analyses focus on the results generated in the final, equilibrium year. The MWBM forcing consists of (a) monthly throughfall $P - E_i$, where P was aggregated from the TRF-HAR forcing files and E_i is the known monthly interception amount for the LSM, and (b) monthly $E_p - E_i$, which is essentially the maximum possible amount of water that the atmosphere can accept from the soil, given that part of the atmospheric demand (E_p) is satisfied by interception loss. A parallel PILPS experiment (termed ''TRF-HARW,'' with the ''W'' referring to an imposed wetted surface) provided the required values of E_p for each month. Because TRF-HARW was effectively identical to TRF-HAR except for the zeroing of all surface resistances to evaporation (equivalent to a ''ponding'' of the soil and leaf surfaces), the evaporation rates it produced are indeed the maximum rates that the atmosphere can accept under the given forcing and can thus be considered the ''potential evaporation'' rates, E_p, for TRF-HAR. The imposed constraints on the energy balance in TRF-HARW led all of the LSMs to produce essentially identical values of E in that experiment, leading to a single set of monthly E_p values for forcing the MWBM.

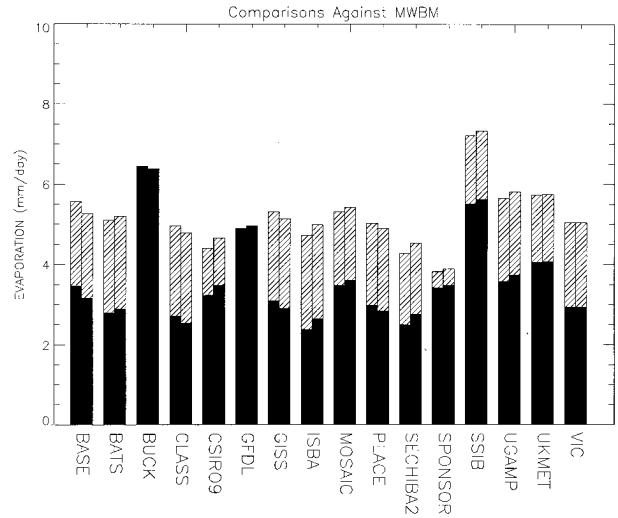

FIG. 3. Reproduction of annual evaporation rates by the MWBM. In each pair of vertical bars, the left bar represents the annual evaporation rate, E_A, from the LSM and the right bar represents E_A as computed by the MWBM. The black section of each bar represents the sum of transpiration and bare soil evaporation, E_w, and the striped section of each bar represents interception loss, E_i. Interception loss is prescribed in the MWBM, and, thus, the striped sections in each pair of vertical bars match perfectly; the test of the MWBM lies in the comparison of the black bars' lengths.

Results on an annual timescale are presented in Fig. 3. The MWBM successfully reproduces the annual E_w values of the different PILPS LSMs. The standard error of estimation for E_w (and thus that for the total annual evaporation, E_A) is 0.16 mm day^{-1}, which is much smaller than the standard deviation of either E_w (1.09 mm day^{-1}) or E_A (0.79 mm day^{-1}) among the LSMs. The square of the correlation coefficient (r^2) between the LSM and MWBM annual E_w values is 0.98, which suggests that the components of the MWBM explain 98% of the variations in LSM E_w. (The corresponding r^2 value for E_A is 0.96.)

Figure 4 shows the seasonal cycles of evaporation produced by the LSMs (solid lines) and the MWBM (dashed lines). The amplitudes of the MWBM's cycles are too large in a few cases (e.g., CLASS and SSIB), and the MWBM's predicted values for individual months (usually March and October) are sometimes poor. Overall, though, the agreement is quite good. The

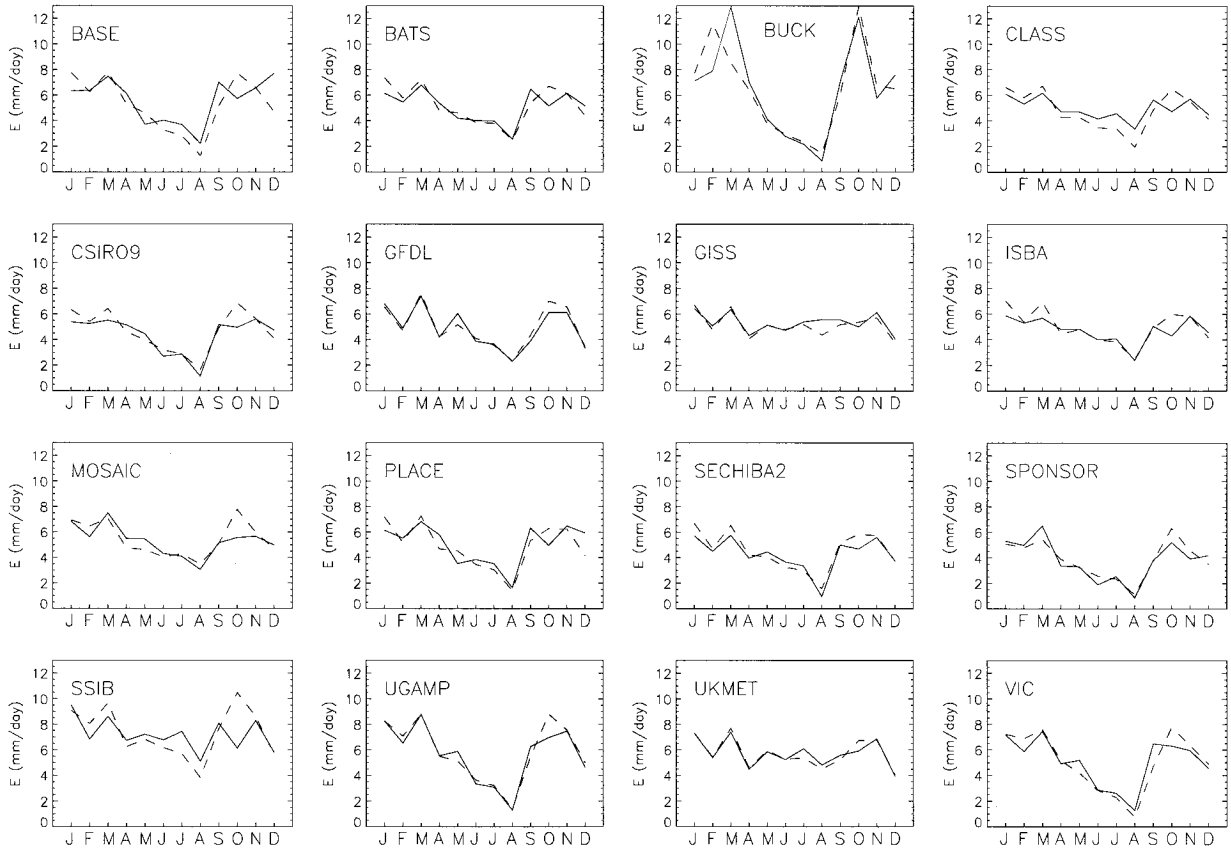

FIG. 4. Comparison of the monthly evaporation rates produced by the PILPS LSMs (solid lines) and the MWBM (dashed lines).

MWBM successully reproduces, for example, the extreme differences in the seasonal cycles produced by UGAMP and UKMET. The standard error of seasonal evaporation estimation by the MWBM is generally about half the standard deviation of the evaporation rates produced for the season by the different LSMs, so by this measure, the MWBM's performance on a seasonal basis is not as strong as it is on an annual basis. Nevertheless, the r^2 values between the PILPS LSM and MWBM seasonal evaporation totals are high, ranging from 0.75 for March–May to 0.89 for June–August. The MWBM also successfully reproduces the seasonal variations of root zone soil moisture content generated by the LSMs (not shown).

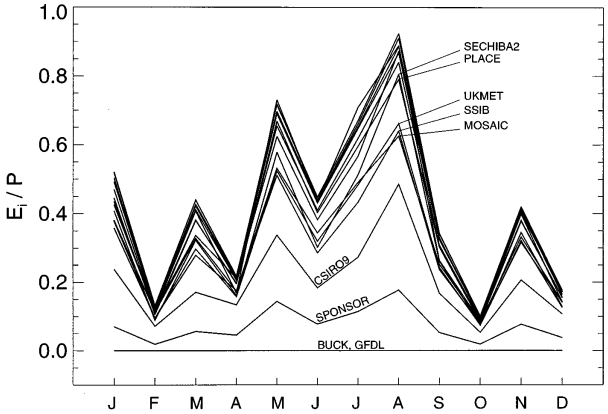

FIG. 5. Monthly ratios of interception loss to precipitation for the PILPS LSMs. Those LSMs with distinct ratios are labeled.

3. Analysis of the PILPS experiment

Overall, the MWBM succeeds in reproducing the annual and seasonal TRF-HAR evaporation rates, given monthly values of precipitation, potential evaporation, and interception loss. Of these three forcing functions, only the last differs significantly among the LSMs. This suggests that the variability in LSM response seen in Fig. 1 can be discussed in terms of differences in interception loss and in the estimated surface runoff, drainage, and evaporation functions [(2)–(9)].

a. Interception loss

Figure 5 shows the monthly ratios of interception loss to precipitation for each PILPS LSM. The BUCK and GFDL LSMs do not explicitly model canopy interception and thus show ratios of zero. The remaining models, except for SPONSOR and CSIRO9, have similar month-

ly ratios. BUCK and GFDL compensate for their lack of interception through the production of large values of E_w, the sum of transpiration and bare soil evaporation (Fig. 3). The E_w generated by SPONSOR, on the other hand, while higher than that of most other LSMs, is not large enough to make up for the low interception loss. SPONSOR thus has the lowest total evaporation of all the LSMs.

b. *Runoff and evaporation: Development of an even simpler characterization*

Differences in the surface runoff, drainage, and evaporation formulations among the LSMs are reflected in the intermodel differences in MWBM parameter values seen in Table 1. A comparison of these parameter values is inherently simpler than a direct comparison of the LSM formulations themselves and can provide some useful insights. We note, for example, that BUCK has the highest m_β value and thus shows the greatest sensitivity of evaporation rate to soil moisture.

The MWBM characterizes each LSM, however, with eight parameters. The effects of intermodel differences in one parameter are often obscured or negated by intermodel differences in another, making an LSM analysis based on a direct comparison of MWBM parameter values still difficult and, at best, convoluted. We therefore further our analysis by finding an even shorter list of quantities that control LSM behavior, each quantity being a unique but simple function of the MWBM parameters and each having a straightforward physical interpretation.

Our short list of two such quantities is introduced in the analysis of the annual water budget presented below. Although this analysis is strictly valid only for those LSMs that do not explicitly model gravitational drainage, we will show that a straightforward generalization of it, covering all LSMs, brings us quite close to our goal of explaining that part of the PILPS intermodel variability associated with differences in soil runoff and evapotranspiration parameterizations.

1) ANALYSIS OF THE ANNUAL MEAN WATER BALANCE

For an LSM that does not compute drainage, the annual mean of the water balance equation, (1), can be combined with (2)–(9) to produce

$$\overline{P} - \overline{E_i} = m_R(\overline{w} - w_R)(\overline{P} - \overline{E_i}) + m_\beta(\overline{w} - w_\beta)(\overline{E_p} - \overline{E_i}). \tag{10}$$

This equation ignores the temporal correlation between soil moisture and the forcing variables, and it ignores the horizontal sections of the R and β_T functions. Solving for $\overline{w}$ and incorporating the solution into (4) and (9) produces an expression for the fraction of throughfall that evaporates rather than runs off:

$$\frac{\overline{E_w}}{\overline{P} - \overline{E_i}} = \frac{m_\beta D + m_R(w_R - w_\beta)m_\beta D}{m_\beta D + m_R}, \tag{11}$$

where D is a climatic parameter related to Budyko's (1974) index of dryness:

$$D = \frac{\overline{E_p} - \overline{E_i}}{\overline{P} - \overline{E_i}}. \tag{12}$$

An alternative expression for this throughfall fraction may have more intuitive appeal and can be easily generalized to include models that compute drainage. Let w_0 and w_1 denote the minimum and maximum values of w, respectively, that the LSM can achieve; these two values bound the "active soil moisture range." The minimum value is that for which E_w goes to zero, since no other moisture sinks are active:

$$w_0 = w_\beta, \tag{13}$$

and the maximum value is that for which all precipitation is converted to runoff:

$$m_R(w_1 - w_R) = 1. \tag{14}$$

With these limits, we can define two useful parameters. The first, $\langle\beta_T\rangle$, is the average value of β_T across the active soil moisture range:

$$\langle\beta_T\rangle = \frac{\int_{w_0}^{w_1} \beta_T \, dw}{w_1 - w_0}. \tag{15}$$

For all models except BUCK (the only LSM that attains a β_T of 1 above a certain critical value of w), this can be rewritten

$$\langle\beta_T\rangle = \frac{1}{2} m_\beta(w_1 - w_\beta). \tag{16}$$

The second parameter, f_R, is the fraction of the active soil moisture range over which runoff occurs:

$$f_R = \frac{w_1 - w_f}{w_1 - w_0}, \tag{17}$$

where w_f is the lowest value of w for which the runoff is positive. For this simple LSM, w_f and w_R are equivalent. Manipulation of (11) with (13)–(17) produces the alternative expression

$$\frac{\overline{E_w}}{\overline{P} - \overline{E_i}} = \frac{2D\langle\beta_T\rangle}{1 + 2D\langle\beta_T\rangle f_R}. \tag{18}$$

2) IMPLICATIONS FOR THE INTERPRETATION OF SOIL MOISTURE

The partitioning of throughfall into runoff and evaporation is indeed a fundamental, if not the most important, calculation of a land surface scheme. If we accept the assumptions that led to (18), namely, the ability of the MWBM to mimic the LSM, the negligibility of

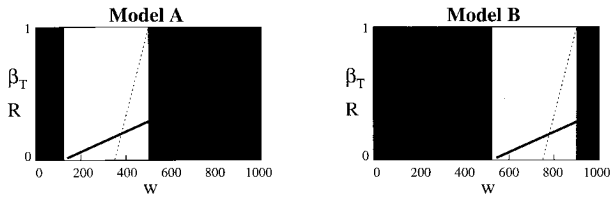

FIG. 6. Contrast of hypothetical LSM formulations for which evaporation and runoff processes act over different soil moisture ranges. Shown are the functions relating root zone soil moisture, w, to β_T (heavy solid line) and surface runoff (dotted line).

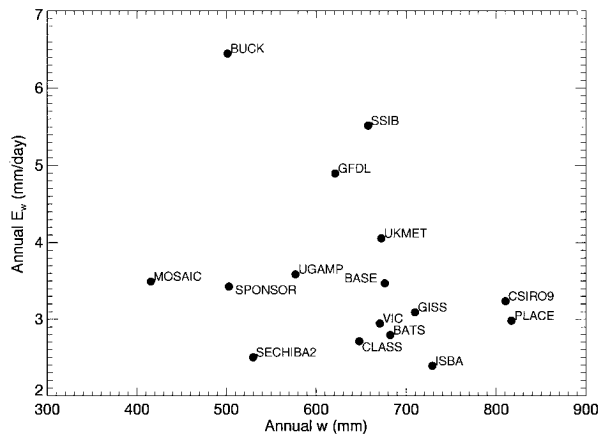

FIG. 7. Variation of annually averaged soil moisture with annual E_w for the various PILPS LSMs.

temporal correlation and nonlinear effects on the annual means, and the absence of subsurface runoff, it follows that this partitioning is a simple function of a climatic parameter, D, and two derived parameters that characterize the β_T and surface runoff functions. We tested the first assumption in section 2b above. The other two will be addressed further in section 3c.

The two derived parameters, $\langle\beta_T\rangle$ and f_R, in fact describe the *relative* positions of the β_T and R functions; the absolute positions are, in a sense, irrelevant in terms of the LSM's response to atmospheric forcing. Consider, for example, the idealized LSMs A and B in Fig. 6. These LSMs have very different active w ranges, and their simulated w values can never match. Nevertheless, the $\langle\beta_T\rangle$ and f_R values for the models are identical, implying an equivalent model response to forcing in the annual mean. In fact, the two models can be shown to produce identical water balances (evaporation rates, runoffs, $w - w_0$, etc.) at every time step under any given forcing when initialized with the same value of $w - w_0$.

By analogy, in a typical PILPS LSM, the soil water balance is controlled only by the relative positions of the effective evapotranspiration, surface runoff, and root-zone drainage curves and not by their absolute positions. We infer that an LSM generating higher absolute values of soil moisture does not necessarily produce higher evaporation rates. An absence of a relation between evaporation and soil moisture among different LSMs has been seen in previous studies (e.g., Desborough et al. 1997; Chen et al. 1997) and is also apparent in the present experiment (Fig. 7).

c. *Application of the simple characterization to the PILPS LSMs*

1) DERIVATION OF $\langle\beta_T\rangle$ AND f_R FOR THE PILPS LSMS

The values of $\langle\beta_T\rangle$ and f_R for the three PILPS LSMs that do not compute significant drainage in this experiment (namely, PLACE, SECHIBA2, and SPONSOR) are determined with (13)–(17), using the parameter values in Table 1. For the remaining LSMs, the definitions of $\langle\beta_T\rangle$ and f_R must be generalized.

The generalization revolves around the redefinition of w_1, the maximum attainable soil moisture. (The definition of w_0 is unchanged; drainage in the PILPS LSMs is never significantly positive at the low end of the active range.) We redefine w_1 to be the value of w for which the maximum precipitation rate from the TRF-HAR forcing (24 mm day^{-1}, a conservatively large value given the monthly timescale) is removed from the system via the sum of R_s and G, as determined with (6) and (7). Thus, at this soil moisture, w does not increase even under the heaviest imposed precipitation. The resulting value of w_1 is fairly robust; the high slopes (m_{G2}) of the drainage functions imply that w_1 is only mildly sensitive to changes in the maximum monthly precipitation. In any case, the derived w_1 value is valid for the TRF-HAR climate, the subject of this paper.

Given w_0 and w_1, $\langle\beta_T\rangle$ is computed with (16). [By necessity, (15) is used for BUCK, even though this particular equation is not fully consistent with (18).] To compute f_R, we set w_f in (17) to the lower of w_R and w_{G2}, the latter being the value of w for which the steeper leg of the G function goes to zero. In other words, f_R is redefined to be the fraction of the active soil moisture range over which either surface runoff or drainage is significantly positive.

Note that the five models computing negative drainage for lower values of w (BATS, GISS, MOSAIC, SSIB, and UKMET) have f_R values that are particularly sensitive to climate, since the strength of recharge in the dry season is a function of the precipitation forcing during the wet season. Due to this recharge, by the way, the dry season E_w values for these models lie well above those of most of the other models (Fig. 4).

Table 2 lists the derived values of $\langle\beta_T\rangle$ and f_R. The values differ widely among the models; $\langle\beta_T\rangle$ varies from 0.125 for ISBA to 0.744 for BUCK, and f_R varies from 0.09 for GISS to 1.00 for MOSAIC and VIC. The limitations imposed by the functional approximations in the MWBM, of course, must always be kept in mind when interpreting these values. For the reasons cited

TABLE 2. Derived values of $\langle\beta_T\rangle$ (dimensionless), f_R (dimensionless), and $w_1 - w_0$ (mm) for each LSM. See caveats in the text regarding the interpretation of these values.

Model	$\langle\beta_T\rangle$	f_R	$w_1 - w_0$
BASE	0.202	0.39	236
BATS	0.171	0.95	194
BUCK	0.744	0.86	332
CLASS	0.231	0.74	466
CSIRO9	0.196	0.61	154
GFDL	0.199	0.18	282
GISS	0.098	0.09	464
ISBA	0.125	0.35	336
MOSAIC	0.237	1.00	192
PLACE	0.139	0.24	182
SECHIBA2	0.132	0.32	142
SPONSOR	0.242	0.99	138
SSIB	0.360	0.50	170
UGAMP	0.257	0.46	258
UKMET	0.166	0.21	458
VIC	0.330	1.00	360

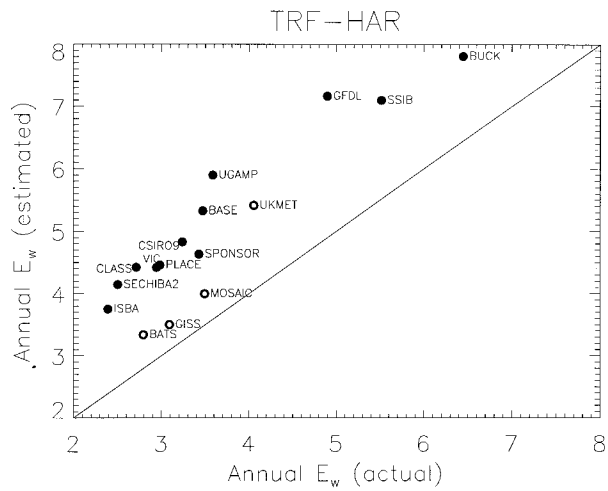

FIG. 8. Comparison of actual and estimated values of E_w for the TRF-HAR experiment. The open circles show the LSMs for which $\langle\beta_T\rangle$ and f_R could not be cleanly derived from the monthly diagnostics.

above, the maximum attainable soil moisture is not well defined for those LSMs that compute drainage. Also, the minimum attainable soil moisture could be significantly lower than w_β; in some LSMs, the ''linear'' relationship between w and β_T appears to break down at the low end. Thus, the difference $w_1 - w_0$ (also shown in the table) is at best a highly approximate representation of the actual active soil moisture range. Furthermore, the scatter in the plotted $\beta_T - w$, $R - w$, and $G - w$ relationships for each LSM (see appendix) can lead to ambiguities in the estimation of the MWBM parameters and thus in the derived $\langle\beta_T\rangle$ and f_R values. Nevertheless, as will be shown in the next section, the estimated values of $\langle\beta_T\rangle$ and f_R do contain important information.

2) ADEQUACY OF EVAPORATION ESTIMATOR

The evaporation estimates generated via (18) with the listed $\langle\beta_T\rangle$ and f_R values are compared to the actual annual evaporation rates in Fig. 8. The equation clearly overestimates the actual annual rates. This positive bias is roughly the same for most LSMs and undoubtedly results from the neglect of temporal correlations and functional nonlinearities in the annual budget analysis. Consider, for example, that for all of the LSMs, soil moistures and precipitation rates are generally highest during the same months. Surface runoff during wet months is thus high for two separate reasons: higher precipitation rates and higher values of R. This positive temporal correlation between soil moisture and precipitation, which tends to increase runoff at the expense of evaporation, is not captured in our analysis of the annual mean water balance and can thus explain, at least in part, the estimation bias. The neglect of the negative correlation between soil moisture and potential evaporation in the annual analysis also promotes the observed positive bias. Another factor is the shape of the assumed piecewise-linear runoff functions. Both R and G are concave upward for most LSMs. Ignoring the horizontal parts of these functions in the annual budget analysis tends to bias runoff estimates downward, raising w and, hence, evaporation.

More important than the evaporation bias, however, is the strength of the correlation between the actual and estimated values of E_w. While the use of the derived $\langle\beta_T\rangle$ and f_R values in (18) strongly compromises analytical rigor given the generalization of these parameters for LSMs that compute drainage, the exercise is clearly instructive—a correlation analysis on the data in Fig. 8 shows that these generalized parameters explain a large portion (84%) of the evaporation variance. Furthermore, a few of the LSMs can be objectively excluded from the analysis. BATS and MOSAIC are the only two LSMs for which significant negative drainage occurs simultaneously with positive surface runoff, so that the f_R values for these two LSMs are ill-defined and are probably overestimated. Also, GISS and UKMET are the only LSMs for which the derived w_0 value lies far below the minimum simulated value of w (by at least 150 mm, more than twice the difference found for any other LSM). Given our data processing algorithms and the assumptions behind (16), the derived $\langle\beta_T\rangle$ and f_R values for GISS and UKMET are probably significantly underestimated. A correlation analysis shows that (18), using the generalized parameters, explains 94% of the intermodel variability over the remaining 12 LSMs.

Thus (18) could serve as a predictor of evaporation rate if we account for the aforementioned positive bias. (The fact that the bias among the LSMs is very similar, especially when we exclude BATS, GISS, MOSAIC, and UKMET from consideration for the reasons cited above, suggests that its magnitude might be predictable, especially because we have identified its probable sources.) More importantly, though, the equation and Fig. 8 demonstrate the usefulness of the parameters $\langle\beta_T\rangle$

and f_R for the characterization of an LSM's water balance formulation. The figure suggests that we can now answer, at least on one level, our original question regarding the sources of intermodel variability in the TRF-HAR experiment—the LSMs generate different evaporation rates because they have different formulations of canopy interception and because differences in the relative positions and shapes of their effective runoff and evaporation functions produce different values of $\langle\beta_T\rangle$ and f_R.

4. Discussion

The analysis in section 2 suggests that the simple relationships comprising the MWBM are behind most of the variations in LSM behavior seen in the TRF-HAR experiment. The further processing of these relationships (section 3) shows that this variability can in fact be discussed in terms of a much smaller set of quantities: the rate of interception loss, the average of β_T over the active soil moisture range ($\langle\beta_T\rangle$), and the fraction of this range over which runoff occurs (f_R). Because the parameters $\langle\beta_T\rangle$ and f_R for a given LSM are determined through curve-fitting exercises rather than through a detailed analysis of the LSM's often complex parameterizations, we do not address here the specific, physics-based reasons for the intermodel $\langle\beta_T\rangle$ and f_R differences; this ''full explanation'' of intermodel variability lies beyond the scope of our study. Rather, we present $\langle\beta_T\rangle$ and f_R as gross yet effective descriptors of an LSM's treatment of soil water dynamics that can shed light on how evaporation and runoff formulations interact in an LSM.

a. Implications for LSM development

Evaporation and runoff formulations are generally the products of separate developmental paths in the construction of an LSM, and, in an LSM's documentation, the two are not often discussed together. Nevertheless, the two formulations must be examined concurrently to produce a clear picture of an LSM's behavior. This is because $\langle\beta_T\rangle$ and f_R are each related to both evapotranspiration and runoff processes. For example, f_R is clearly related to the LSM's runoff formulation but is also affected by the evapotranspiration formulation through the definition of the lower bound of the active soil moisture range. Similarly, the surface runoff and drainage parameterizations define the upper bound of the range and thereby exert a strong influence over $\langle\beta_T\rangle$.

We can thus conclude that the nature of a β_T curve is not important by itself for determining realistic evaporation rates. The interaction between this curve and the runoff curves is also important; the formulations of surface runoff and drainage determine the maximum attainable soil moisture and thus the active part of the β_T curve.

The dual importance of evaporation and runoff processes implies a need for a balanced representation of energy fluxes and water balance fluxes in an LSM. The importance of this balance is now demonstrated with an MWBM sensitivity study. Assume for the sake of argument that the β_T curve in Fig. 9a (the solid line) is ''perfect''—that is, a completely realistic representation of how transpiration efficiency (in terms of stomatal conductance, etc.) responds to root zone soil moisture. We allow the curve to level off to a constant value at higher values of w in order to show that our arguments apply beyond the constraints of the simple MWBM framework. (Again, the leveling off is presumably an inherent part of many LSMs, though it was not clearly seen in the TRF-HAR diagnostics.)

Now consider the dotted lines A–D in Fig. 9a, which represent four possible R formulations. The MWBM, after being modified to handle the β_T curve's revised shape, was integrated under TRF-HAR forcing four times, once for each of the four R curves. Figure 9b shows that the resulting evaporation rates generated in the dry season (June–August, or JJA) are indeed quite sensitive to the positions of these curves. The line D produces the largest evaporation rate, which is not surprising given that it produces the highest $\langle\beta_T\rangle$ and the lowest f_R. Note that the imposed R variations are much smaller than those seen among the PILPS LSMs (Table 1).

Another series of sensitivity tests is illustrated in Fig. 9c. The four assumed values of f_R, which span the range seen among the PILPS LSMs, also result in significantly different dry season evaporation rates (Fig. 9d). Note that an LSM's effective f_R is determined in part by the treatment of soil moisture heterogeneity; those LSMs that account for saturated subgrid patches of a grid cell and the associated generation of storm runoff over these patches will have higher values of f_R.

In short, the effectiveness of a ''perfect'' β_T curve could be severely limited by errors in the formulation of surface runoff and drainage (and thus in $\langle\beta_T\rangle$ and f_R). Assuming that a proper β_T curve does indeed level off at higher values of w, the evaporation errors associated with the runoff formulation will be most pronounced during times of water stress.

We note in passing that the physical mechanisms controlling transpiration and runoff generation in the real world are, in principle, similarly connected to each other through available soil moisture. The extraction of $\langle\beta_T\rangle$ and f_R from observational datasets, not necessarily a simple task, could perhaps serve as a starting point for analyzing this interaction and comparing it to that inherent in LSMs.

b. Generalization of results

The analyses have focused on the TRF-HAR experiment to avoid variations in the treatment of albedo, turbulence, and spatial heterogeneity in vegetation among the PILPS LSMs and thus to isolate more clearly

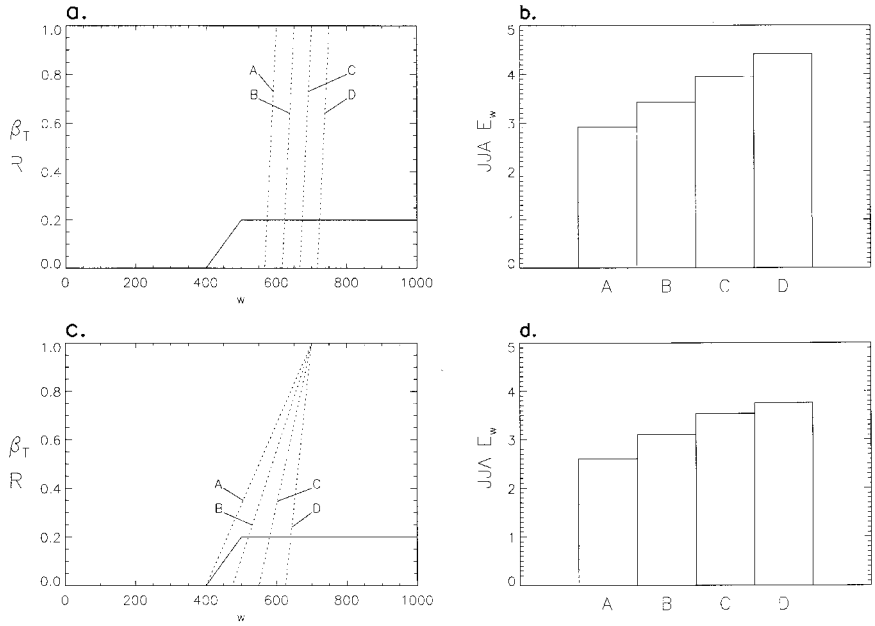

FIG. 9. (a) Assumed β_T curve (solid) and R curves (dashed) for the first set of MWBM sensitivity experiments. (b) Resulting JJA evaporation rates (mm day^{-1}). (c) Assumed β_T curve (solid) and R curves (dashed) for the second set of MWBM sensitivity experiments. (d) Resulting JJA evaporation rates (mm day^{-1}).

the controls of evaporation and runoff processes on LSM behavior. To be useful, however, the results must be generalized to a less restrictive experiment. We therefore repeated the analyses in sections 2 and 3 using data from the PILPS ''TRF-H'' experiment, which is equivalent to the TRH-HAR experiment except that it allows the LSMs to compute their own albedo and turbulent transfer coefficients. We maintain, however, the imposition of 100% canopy cover, since for this condition we have appropriate estimates of potential evaporation—values of E_p for a given LSM were set to the evaporation rates generated by that LSM in the TRF-HW experiment, which was equivalent to the TRF-H experiment except for the removal of all surface resistances to evaporation. Note that the specification of LSM-specific E_p time series implies that this analysis still does not address the controls over these rates; the determination of E_p, like interception loss, is external to the MWBM.

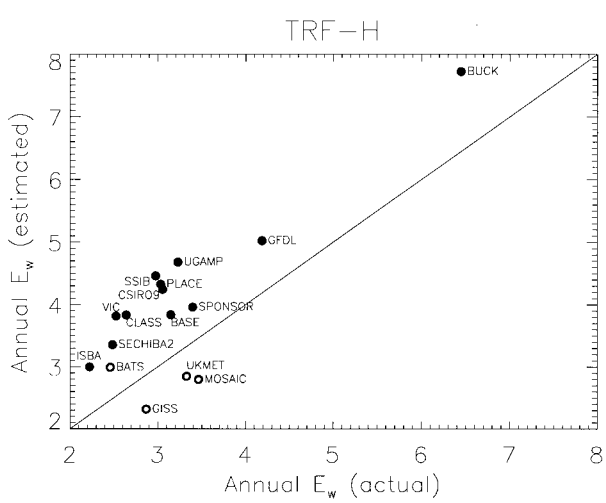

FIG. 10. Comparison of actual and estimated values of E_w for the TRF-H experiment. The open circles show the LSMs for which $\langle\beta_T\rangle$ and f_R could not be cleanly derived from the monthly diagnostics.

The MWBM (with new values for its parameters) again accurately reproduces the annual E_w values generated in this experiment, with an r^2 of 0.97 and a standard error of estimation of 0.24 mm day^{-1}. (The standard deviation of annual E_w among the LSMs in the TRF-H experiment is 0.96 mm day^{-1}.) Figure 10 shows how E_w computed with (18) compares with the actual rates in the TRF-H experiment; again, though the scatter is a bit higher than in Fig. 8, $\langle\beta_T\rangle$ and f_R remain the important controls on E_w, particularly when BATS, MOSAIC, GISS, and UKMET are excluded from the analysis for the reasons cited in section 3c. We conclude that the results in sections 2 and 3 are not specific to the more restrictive TRF-HAR experiment.

The annual evaporation rates generated by the PILPS LSMs in the TRF-H experiment, by the way, were generally about the same or a little lower than those generated in TRF-HAR. SSIB, however, showed a very large decrease in evaporation. The somewhat artificial controls imposed on SSIB in TRF-HAR apparently had a profound effect on its behavior.

5. Summary

We emphasize that the monthly water balance model (MWBM) is not being introduced here as a potential substitute for more complex land surface models (LSMs) in climate studies. The functional relationships fitted for the MWBM are the net, effective result of more physically based parameterizations, and the examination of the same vegetation type under different conditions would lead to changes in these relationships that cannot be predicted a priori. (Indeed, the fitted MWBM parameters presented in Table 1 are consistent with the LSMs' response to imperfect GCM forcing over the Amazon and might not describe the LSMs' behavior under less extreme conditions. These particular values are in any case subject to error given their derivation from monthly diagnostics.) Operational use of the MWBM is further limited by the prescription, rather than prediction, of interception loss and potential evaporation and by complications associated with snowfall and seasonally varying vegetation characteristics.

We instead introduce the MWBM as a tool for understanding the differences in evaporation rates shown in Fig. 1 and, in particular, for understanding how the interplay between evaporation and runoff formulations affects simulated soil water dynamics. The MWBM successfully reproduces the evaporation rates of each of the sixteen PILPS LSMs (Figs. 3 and 4). This implies that we can relate much, if not most, of the evaporation differences in Fig. 1 differences in MWBM parameter values—that is, to different interception loss rates and different functional relationships between root zone soil moisture and (a) transpiration efficiency (β_T), (b) surface runoff generation, and (c) root-zone drainage generation.

These different functional relationships can in turn be represented very simply by two derived parameters: (a) the average of the β_T function across the active soil moisture range, $\langle\beta_T\rangle$, and (b) the fraction of this range over which runoff can form, f_R. We have, in fact, shown that the intermodel variability in Fig. 1 for the PILPS TRF-HAR experiment can be discussed in terms of intermodel variations in interception loss and in these two parameters. If we know $\langle\beta_T\rangle$ and f_R for a given LSM, and if we can characterize the climate in terms of an index of dryness (as modified by known interception loss rates), we can predict the annual ratio of soil water evaporation to applied throughfall using (18) alone—that is, without detailed knowledge of the LSM's formulations, which may be very complex.

The values of $\langle\beta_T\rangle$ and f_R in an LSM are determined by the shapes and relative positions of the LSM's effective β_T, R, and G functions, that is, by the nature of soil moisture's simultaneous control over evaporation and runoff. We infer that one requirement for an accurate simulation of a region's water budget (and thus energy budget) is compatibility between the LSM's evaporation and runoff formulations. The simple sensitivity experiments in Fig. 9 demonstrate that even a ''perfect'' description of canopy structure and stomatal behavior, toward which many LSMs strive, does not ensure realistic evaporation rates if the runoff formulation remains relatively crude or incompatible with the evaporation formulation. Understanding the interaction between evaporation and runoff processes in an LSM—understanding, for example, how runoff processes affect soil moistures and thereby the active part of the effective β_T curve—is critical to a full understanding of the LSM's behavior.

Acknowledgments. Krista Dunne's assistance in managing the PILPS LSM output files proved invaluable. The many PILPS participants who contributed datasets to this study are gratefully acknowledged; indeed, these contributors made the study possible. They include A. J. Pitman, A. Henderson-Sellers, F. Abramopoulos, A. Boone, C. E. Desborough, R. E. Dickinson, J. R. Garratt, N. Gedney, A. Hahmann, E. Kowalczyk, K. Laval, D. Lettenmaier, X. Liang, J.-F. Mahfouf, J. Noilhan, J. Polcher, W. Qu, A. Robock, C. Rosenzweig, C. A. Schlosser, A. B. Shmakin, J. Smith, M. Suarez, D. Verseghy, P. Wetzel, E. Wood, Y. Xue, and Z. L. Yang. For many constructive comments on the manuscript, we thank A. Pitman, C. Desborough, A. Schlosser, A. Robock, Z. Liang, P. Wetzel, R. Dickinson, and two anonymous reviewers.

APPENDIX

Estimation of Parameters

Here we describe the estimation of the MWBM parameters from the monthly diagnostic files generated by each PILPS LSM for experiment TRF-HAR.

a. Interception loss

Each PILPS participant provided monthly interception loss rates as part of the submitted diagnostic data. We simply assigned these values of E_i to the MWBM.

b. Runoff fraction

Monthly values of surface runoff (R_s) and interception loss provided in the PILPS diagnostics can be combined with monthly precipitation rates from the TRF-HAR forcing data to generate values of runoff fraction:

$$R = \frac{R_s}{P - E_i}. \tag{A1}$$

A few of the LSMs (e.g., GISS and ISBA) allow a horizontal moisture flow out of the root zone in addition to surface runoff; for our purposes, this flow is added to the surface runoff.

Because the monthly mean root zone soil moisture w is also included in the PILPS diagnostics, we can con-

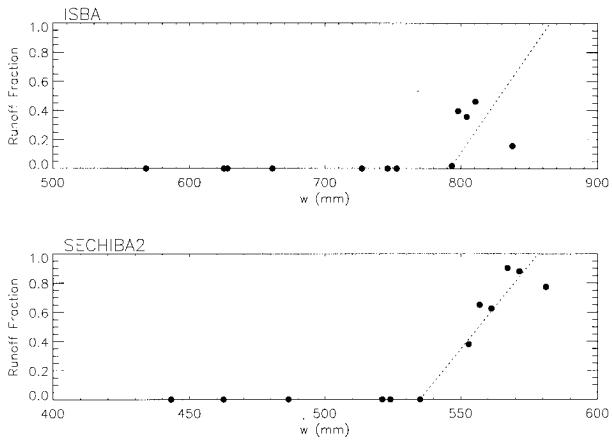

FIG. A1. Variation of runoff fraction, R, with root zone soil moisture, w, for two representative PILPS LSMs.

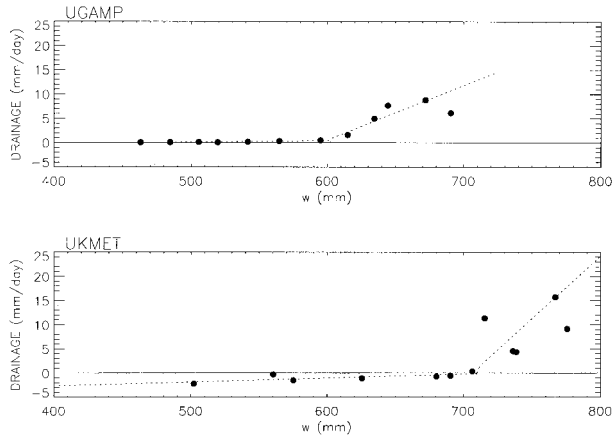

FIG. A3. Variation of root-zone drainage rate with root zone soil moisture, w, for two representative LSMs.

struct a plot of R versus w for each LSM. Figure A1 shows, for a couple of representative models, some scatter from a pure monotonic, curvilinear relationship. This scatter has at least two sources. First, the root-zone soil moisture might not adequately reflect the moisture in a thin surface layer, which many LSMs model explicitly and use in their runoff parameterizations. Second, the averaging process may introduce important biases; if the effective R function in an LSM is nonlinear in w, and if w_{inst} (the instantaneous, or time step, value of w) varies over a given month, then we have the inequality:

$$R(\overline{w_{\text{inst}}}) \neq \overline{R(w_{\text{inst}})}, \tag{A2}$$

where the overline indicates an averaging over the month.

Despite the scatter, the relationship between R and soil moisture is strong enough in Fig. A1 and in the corresponding plots for the other LSMs to allow an estimation, for each LSM, of m_R and w_R through a simple fitting technique that is both fully objective and capable of working with a very small number of points. (We did not use linear regression because in some cases, only three or four points were available for fitting.) The technique is illustrated in Fig. A2. Figure A2a shows the A2 monthly runoff ratios as a function of w for a hypothetical LSM. We determine the highest soil moisture for which R is still smaller than a small critical value (0.05 in our analysis); this is shown as Point A in Fig. A2b. We then connect the points at higher soil moistures and determine the area under the resulting curve—that is, the area of the shaded region in Fig. A2b. The fitted slope and intercept for this set of runoff ratios are those values that describe the top of the trapezoid in Fig. A2c, which has the same area, and which begins and ends at

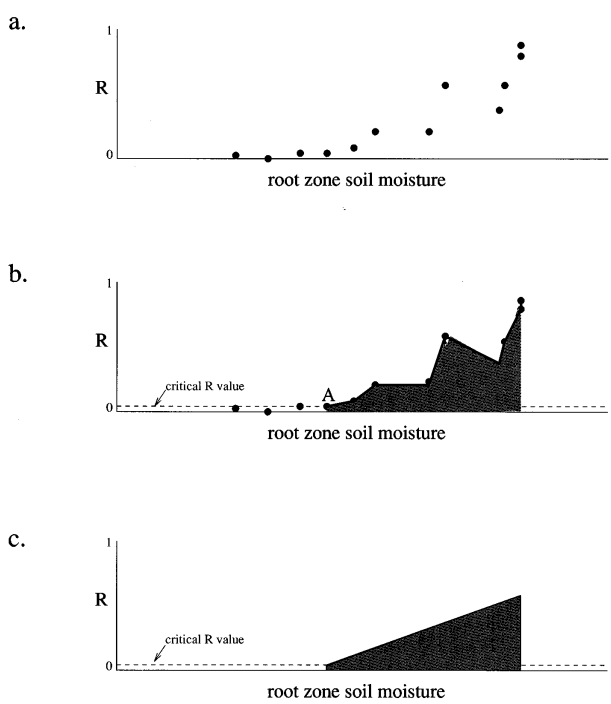

FIG. A2. Fitting procedure applied to generate the functional relationships used by the MWBM.

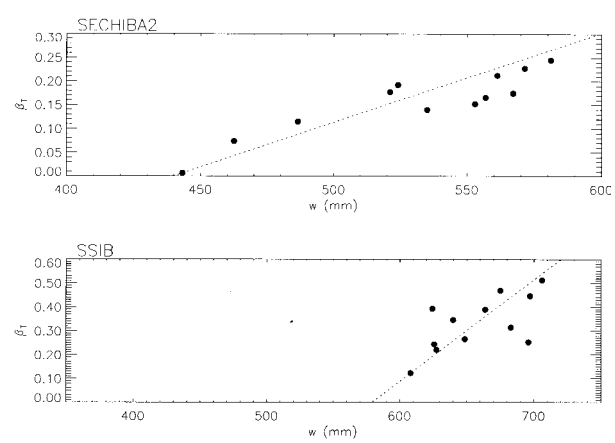

FIG. A4. Variation of β_T with root zone soil moisture, w, for two representative PILPS LSMs.

the same soil moistures, as the shaded region in Fig. A2b. For models that never produce surface runoff, m_R and w_R are set to zero. The derived R functions for the ISBA and SECHIBA2LSMs are shown as dashed lines in Fig. A1.

c. Root-zone drainage

The submitted PILPS diagnostic files provide monthly values of G, the flow of moisture across the bottom of the root zone. Figure 13 shows a plot of G versus w for two representative LSMs. The highly nonlinear nature of the effective $G(w)$ functions is readily apparent. For UKMET, G is in fact negative for w below about 700 mm, presumably reflecting the existence of a lower soil reservoir (deeper than the root zone) that can provide moisture to the root zone during dry periods.

As suggested by (7), the effective $G(w)$ function for each LSM is approximated by the juxtaposition of two lines in each plot, one derived from the points for which $w < w_{G2}$, and the other derived from the points for which $w > w_{G2}$. (These are shown as dashed lines in Fig. A3.) For this analysis, w_{G2} is arbitrarily set to the highest monthly value of w for which the LSM still produces a G less than 1.0 mm day^{-1}.

The procedure described in Fig. A2 is used to estimate m_{G2}. The trapezoid, however, is collapsed into a triangle with the base on the axis itself. On the left side of w_{G2}, to capture the upward, dry season recharge that occurs in some LSMs, linear regression is used to estimate m_{G1} and w_{G1}. For models having no drainage at all, m_{G1}, w_{G1}, m_{G2}, and w_{G2} are set to zero.

d. Transpiration efficiency

The submitted PILPS diagnostic files include monthly values of E_i and total evaporation, E $(= E_i + E_w)$. Combining these with estimates of monthly potential evaporation (E_p) from the TRF-HARW experiment (see section 2b) produces, for each month, an estimate for the effective transpiration efficiency:

$$\beta_T = \frac{E - E_i}{E_p - E_i}. \tag{A3}$$

Figure A4 shows how β_T varies with w for two representative PILPS LSMs. As expected, β_T generally increases with w, with scatter from a pure monotonic relationship probably resulting from (a) monthly variations in other factors that control transpiration efficiency, such as vapor pressure deficit stress, and (b) the use of monthly diagnostics, leading to nonlinearity effects analogous to those embodied in (A2). The relationship with soil moisture is strong enough in Fig. 14 and in the corresponding plots for the other LSMs to allow an estimation, for each LSM, of m_β and w_β through the technique illustrated in Fig. A2, using a critical β_T value of 0.02. The derived functions for SECHIBA2 and SSIB are shown as dashed lines in Fig. A4.

Note that for SECHIBA2, w has a lower bound of about 440 mm, since transpiration ceases at this point. In addition, all precipitation in SECHIBA2 is converted to surface runoff when w reaches approximately 580 mm (Fig. A1), and thus 580 mm serves as an upper bound for SECHIBA2's root-zone soil moisture. SECHIBA2 therefore experiences its full range of soil moisture conditions during the TRF-HAR experiment. For the PILPS LSMs, in general, the wet and dry seasons in the TRF-HAR experiment generate the broad range of wetness conditions needed to allow the estimation of the various MWBM parameters.

REFERENCES

Abramopoulos, F., C. Rosenzweig, and B. Choudhury, 1988: Improved ground hydrology calculations for global climate models (GCMs): Soil water movement and evapotranspiration. *J. Climate,* **1,** 921–941.

Budyko, M. I., 1974: *Climate and Life.* Academic Press, 508 pp.

Chen, T. H., and Coauthors, 1997: Cabauw experimental results from the Project for Intercomparison of Land-surface Parameterization Schemes (PILPS). *J. Climate,* **10,** 1194–1215.

Cuenca, R. H., M. Ek, and L. Mahrt, 1996: Impact of soil water property parameterization on atmospheric boundary layer simulation. *J. Geophys. Res.,* **101,** 7269–7277.

Desborough, C. E., 1997: The impact of root-weighting on the response of transpiration to moisture stress in land surface schemes. *Mon. Wea. Rev.,* **125,** 1920–1930.

——, A. J. Pitman, and P. J. Irannejad, 1996: Analysis of the relationship between bare soil evaporation and soil moisture simulated by 13 land surface schemes for a simple non-vegetated site. *Global Planet. Change,* **13,** 47–56.

Dickinson, R. E., A. Henderson-Sellers, and P. J. Kennedy, 1993: Biosphere–Atmosphere Transfer Scheme (BATS) Version 1e as coupled to the NCAR community climate model. NCAR Tech. Note NCAR/TN-387+STR, 72 pp. [Available from National Center for Atmospheric Research, P. O. Box 3000 Boulder, CO 80307.]

Ducoudre, N. I., K. Laval, and A. Perrier, 1993: SECHIBA, a new set of parameterizations of the hydrologic exchanges at the land/atmosphere interface within the LMD atmospheric general circulation model. *J. Climate,* **6,** 248–273.

Gedney, N., 1996: *Development of a Land Surface Scheme and its Application to the Sahel.* University of Reading, 200 pp.

Gregory, D., and R. N. B. Smith, 1994: Canopy, surface and soil hydrology. Unified Model Documentation Paper 25, 19 pp. [Available from U.K. Meterological Office, London Road, Bracknell RG12 2SZ, England.]

Henderson-Sellers, A., Z.-L. Yang, and R. E. Dickinson, 1993: The Project for Intercomparison of Land-surface Parameterization Schemes. *Bull. Amer. Meteor. Soc.,* **74,** 1335–1349.

Koster, R. D., and M. J. Suarez, 1996: Energy and water balance calculations in the Mosaic LSM. NASA Tech. Memo. 104606, Vol. 9, 59 pp. [Available from NASA/Center for Aerospace Information, 800 Elkridge Landing Road, Linthicum Heights, MD 21090.]

Kowalczyk, E. A., J. R. Garratt, and P. B. Krummel, 1991: A soil-canopy scheme for use in a numerical model of the atmosphere—1D stand-alone model. CSIRO Division of Atmospheric Research Technical Paper 23, 56 pp. [Available from CSIRO Division of Atmospheric Research, Aspendale, Victoria, Australia.]

Liang, X., D. P. Lettenmaier, E. F. Wood, and S. J. Burges, 1994: A simple hydrologically-based model of land surface water and

energy fluxes for general circulation models. *J. Geophys. Res.,* **99,** 14 415–14 428.

——, E. F. Wood, and D. P. Lettenmaier, 1996: Surface soil moisture parameterization of the VIC-2L model: Evaluation and modifications. *Global Planet. Change,* **13,** 195–206.

Milly, P. C. D., 1992: Potential evaporation and soil moisture in general circulation models. *J. Climate,* **5,** 209–226.

Noilhan, J., and S. Planton, 1989: A simple parameterization of land surface processes for meteorological models. *Mon. Wea. Rev.,* **117,** 536–549.

Pitman, A., and Coauthors, 1993: Project for Intercomparison of Land-surface Parameterization Schemes, Results from offline control simulations (Phase 1a). International GEWEX Project Office Publication Series No. 7, GEWEX/WCRP, 47 pp. [Available from International GEWEX Project Office, 1100 Wayne Avenue, Suite 1210, Silver Spring, MD 20910.]

Polcher, J., K. Laval, L. Dumenil, J. Lean, and P. R. Rowntree, 1996: Comparing three land surface schemes used in general circulation models. *J. Hydrol.,* **180,** 373–394.

Robock, A., K. Ya. Vinnikov, C. A. Schlosser, N. A. Speranskaya, and Y. K. Xue, 1995: Use of midlatitude soil moisture and meteorological observations to validate soil moisture simulations with biosphere and bucket models. *J. Climate,* **8,** 15–35.

Shmakin, A. B., A. Yu. Mikhailov, and S. A. Bulanov, 1993: Parameterization scheme of the land hydrology considering the orography at different spatial scales. *Exchange Processes at the Land Surface for a Range of Space and Time Scales,* H.-J. Bolle, R. A. Feddes, and J. D. Kalma, Eds., IAHS, 569–575.

——, O. N. Nasonova, and Y. M. Gusev, 1996: Relative importance of some processes description in the soil-vegetation-atmosphere transfer modeling (results of PILPS-type experiments). Preprints, *Second Int. Scientific Conf. on the Global Energy and Water Cycle,* Washington, DC, GEWEX-WCRP, 168–169.

Sud, Y. C., and M. J. Fennessy, 1982: An observational-data based evapotranspiration function for general circulation models. *Atmos.–Ocean,* **20,** 301–316.

Verseghy, D. L., N. A. McFarlane, and M. Lazare, 1993: CLASS—A Canadian land surface scheme for GCMs, II. Vegetation model and coupled runs. *Int. J. Climatol.,* **13,** 347–370.

Wetzel, P. J., and A. Boone, 1995: A parameterization for land–atmosphere–cloud exchange (PLACE): Documentation and testing of a detailed process model of the partly cloudy boundary layer over heterogeneous land. *J. Climate,* **8,** 1810–1837.

——, X. Liang, P. Irannejad, A. Boone, J. Noilhan, Y. Shao, C. Skelly, Y. Xue, and Z. L. Yang, 1996: Modeling vadose zone liquid water fluxes: Infiltration, runoff, drainage, interflow. *Global Planet. Change,* **13,** 57–71.

Xue, Y., P. J. Sellers, J. L. Kinter, and J. Shukla, 1991: A simplified biosphere model for global climate studies. *J. Climate,* **4,** 345–364.